

A NEW METHOD OF TESTING THE HETEROGENEITY OF THE IMPACT ORIGIN, SHATTER CONES OF NEWLY DISCOVERED IMPACT SITE, SANTA FE NEW MEXICO, USA. T. Adachi^{1,2} and G. Kletetschka^{1,2,3,1}
 Department of Physics, Catholic University of America, 200 Hannan Hall, Washington DC, USA (Tomoko.Adachi-1@nasa.gov), ²NASA Goddard Space Flight Center, Code 691, Greenbelt, MD, USA (gkletetschka@nasa.gov), ³Institute of Geology, Academy of Sciences of the Czech Republic, Prague, Czech Republic).

Abstract: A meter scale shatter cone structures were found in the Sangre De Cristo Mountains near Santa Fe, New Mexico. The possible impact deformed rocks are consist of Proterozoic biotite schist and granite. Well pronounced shatter cone structures are pervasive throughout the outcrops. The impact origin can be tested a line of magnetic analysis and a new method of magnetic scanning for 2-dimentional imaging. Along with magnetic signature analysis, the magnetization orientation may be a proxy indicator for an impact origin.

Previous study on a suite of rocks from Sierra Madera, Texas showed the impact pressure controlled magnetization orientations. We characterized the magnetic signatures of two distinct physical characteristics of shock fractured rocks, A: small scale, and B: large scale shatter cones. The magnetic signatures of the two shatter cones showed the heterogeneous orientations and intensity of natural remanent magnetizations that may attribute to the impact event (Figure 1 & 2).

Along with the conventional magnetic analysis, a new method of magnetic scanning gives us another line of proxy indicator for impact origin.

Introduction: The Sierra Madera Impact crater is located in Pecos county, Texas, USA. It is a complex impact crater with an intensely folded and faulted central uplift [1][2]. It had been initially described by [3] and [4]. The shock pressure was estimated as ~40 (central uplift) GPa by [5]. Huson et al. [6] estimated 8 to 30 GPa using X-ray powder diffraction (XRD) analysis of shatter cones. Sharpness of the peaks in the XRD pattern indicate crystallinity, and asymmetric broadening in the XRD patterns indicates spatial inhomogeneity due to shock effects [7].

We performed magnetic analyses for two localities of Sierra Madera impact deformed rocks that have different physical characteristics of shock deformation. The magnetic signatures of the two locations, sites A and B showed the distinct magnetic signatures. Shatter cone at site A has a fine-scale (few to ~10 mm) distributed array of complete shatter cones with sharp apex. Natural remanent magnetization (NRM) of site A shatter cone is distributed within the plane that is perpendicular to the apexes of the cones. Shatter cone at site B shows no apparent cone shape or apex, instead, a relatively larger scale and multiple striated

joint set (MSJS) and sinusoidal continuous peak. NRM of site B shatter cone is clustered along the apexes. The difference in magnetization direction is a likely indicator of the shock pressure where parallel to apex indicates pressures larger than 10 GPa and perpendicular to apex indicate pressures less than 10 GPa. Intensities of NRM and saturation isothermal remanent magnetization (SIRM) contrast and fluctuate within a shatter cone as well as in between two sites. We observed a random orientation of magnetic vector directions and amplitudes changing over small scales, leading to the absence of coherent macro-scale signature.

Impact magnetization and demagnetization:

Hypervelocity impact produces an amount of energy that deforms, fractures, and melts the target rocks. Hargraves and Perkins [8] used magnetic techniques to study rocks affected by shock induced high strain rate deformation. The noted effects of impacts were: changes in NRM directions, remagnetization, and reduction in bulk susceptibility. An important finding was that the impact effect on NRM was detectable. Shock remanent magnetization (SRM) collectively includes various effects that must be identified: demagnetization and/or remagnetization which may involve changes in magnetic remanence directions. The mechanism of shock induced magnetic effects (SRM) in shatter cones has not been satisfactory explained. [9] suggested the relatively late formation of shatter cone structures in the Vredefort impact crater during the impact compression. [10] suggested the high remanent magnetism over the Vredefort impact structures is due to elongated, micron-size single-domain magnetite that formed along PDFs under extreme P-T conditions. In their studies magnetizations of shatter cones were not considered.

Method: The magnetic characterization was designed to observe small-scale (centimeters) heterogeneity in magnetism possibly recorded at an impact event. The Sierra Madera shatter cone samples were prepared to preserve orientations and spatial configurations. Shatter cone sub-samples were cut out into cubes from A: 1.2 to B: 1.5 cm³ in order to preserve the spatial orientation of each other respect to the parent sample, and the orientations of the apex axis. The orientations of the apex axis were kept to be parallel to the z-axis of the magnetometer with the errors ranging ± 5 degrees. The sub-samples of A were cut out and labeled as: A1, A2, A3, through A10, and eight out of ten of them were

used for analysis. A1 and A2 were basal (below apex, no striations), and A3 through A10 were with apex structures with striations, and re-crystallized surfaces. The sub-samples of B were cut out and labeled as B1, B2, B3 though B10. B1 through B7 are basal (below apex and no striations), and B8, B9a, and B10 has multiple striated joint set.

With the orientation maintained throughout the analysis, natural remanent magnetization (NRM), alternating field demagnetization (AF-demag), and saturation magnetization (SIRM) were performed.

Results: Small scale shatter cone A: Fig. 3 shows that the fluctuation of NRM (solid squares) values has bimodal distribution, where samples A1, A2, A4, A6, and A10 are $1 \text{ to } 2 \times 10^{-7} \text{ Am}^2/\text{kg}$, while A3, A5, and A7 are $6 \text{ to } 7 \times 10^{-7} \text{ Am}^2/\text{kg}$. SIRM (open squares) values are narrowly distributed within $3 \text{ to } 5 \times 10^{-5} \text{ Am}^2/\text{kg}$.

Large scale shatter cone B: Fig. 3 shows a relatively uniform distribution of NRM ($0.5 \text{ to } 0.9 \times 10^{-6} \text{ Am}^2/\text{kg}$) (solid squares) except B9a and B10 (ridgeline apex) show slightly higher values ($1 \text{ to } 2 \times 10^{-6} \text{ Am}^2/\text{kg}$). Whereas the SIRM (open squares) shows bimodal distribution where B4 and B6 have order of magnitude lower SIRM ($1.17 \times 10^{-5} \text{ Am}^2/\text{kg}$ and $1.60 \times 10^{-5} \text{ Am}^2/\text{kg}$), respectively, compared with $1 \text{ to } 4 \times 10^{-4} \text{ Am}^2/\text{kg}$ for the rest of the B-samples.

The NRM values of B are similar to the higher NRM values of A (A3, A5, A7). These fluctuations are reflected in the REM (magnetic efficiency) values (solid triangles). The overall efficiency (averaged REM values of all the sub-samples) is ~ 0.005 , which is lower than suggested terrestrial NRM values of 0.01 [11] [12] However, the efficiency of B4 (0.06) and B6 (0.05) is much higher than the rest of the samples or common terrestrial values.

The vector orientations as declination (x-axis) versus inclination (y-axis) were plotted in Fig. 1 for A, and Fig. 2 for B, to depict the vector behaviors. The NRM fluctuations of shatter cone A shows that most of the vectors except A4 and A6 are oriented perpendicular to the shatter cone axes that is normal to the base. The NRM directions in shatter cone B clusters in about 70° inclination, and parallel to shatter cone axis as in Fig. 4.

Application: We test the result of the heterogeneity of the magnetic signatures of the Sierra Madera shatter cones by using 2-D magnetic scanning method to depict the orientation and intensity of the magnetizations of Sierra Madera shatter cone, and apply for the newly discovered impact site, Santa Fe possible impact site to test the origin of the shatter cone rocks.

References: [1] Wilshire et al. (1971) *GSA Bulletin*, v.82, p1009-&. [2] Wilshire et al (1972) *USGS*

Prof. Paper, v.599-H, p.1-49. [3] Boon and Albritton, Jr. (1936) *Field and Laboratory*, v.5, p.1-9. [4] Eggleton and Shoemaker (1961) *USGS Prof. Paper*, v.424-D. [5] Goldin et al. (2005) *LPSC XXXVI*, 1071. [6] Huson et al. (2006) *LPSC*. [7] Ashworth and Schneider (1985) *Physics and Chemistry of Minerals*, v.11, p.241-249. [8] Hargraves and Perkins (1969) *JGR*, v.74, p.2576-2589. [9] Nicolaysen and Reimold (1999) *JGR-Solid Earth*, v.104, p.4911-4930. [10] Hart et al. (2000) *Geology*, v.23, p.277-280. [11] Kletetschka et al. (2003a) *Meteoritics & Planetary Science*, v.38, p.1-last. [12] Kletetschka et al. (2003b) *The Leading Edge*.

Figure 1:

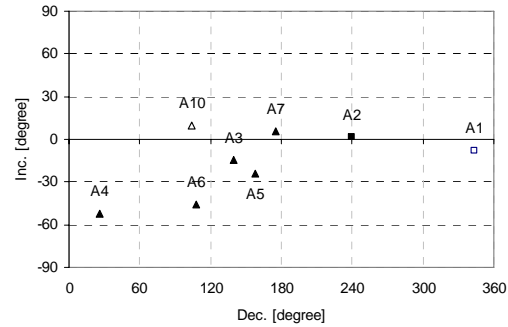


Figure 2:

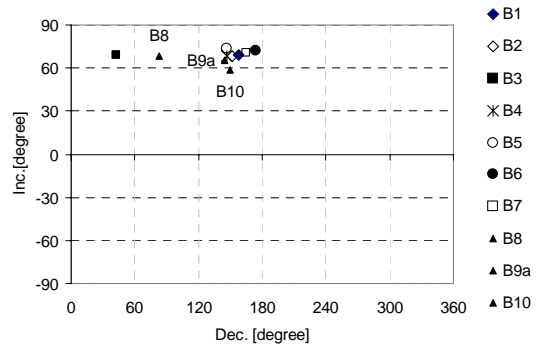


Figure 3:

